Enhancement of Multifrequency Microwave Tomography Breast Imaging System using Flexible Preconditioner Based Krylov Subspace Methods

N. Nithya and M. S. K. Manikandan

Department of Electronics and Communication Engineering
Thiagarajar College of Engineering, Madurai 625015, India
nithyan@student.tce.edu, manimsk@tce.edu.

Abstract **–** Microwave Tomography Imaging System (MwTIS) is an emerging tool for medical diagnosis in the non-invasive screening process. This paper addresses the ill-condition problem by proposing two new schemes incorporated into the DBIM image reconstructed algorithm for high frequencies in MwTIS. The first scheme is to propose an optimal step frequency using the degree of ill-posedness value for reducing the frequency diversity problem. The second scheme is to propose Krylov Subspace-based regularization method called Flexible Preconditioned Conjugate Gradient Least Square (FP-CGLS) method to resolve the ill-condition problem. The iteratively updated preconditioner matrix in the proposed FP-CGLS method reduces the number of iterations and it is stable in high-level Gaussian noise. The efficiency of the proposed FP-CGLS method is validated by imposing Gaussian noise up to 30% in scattered breast phantom in the multifrequency range of 2 GHz -3 GHz It achieves an enhanced reconstructed image at 12 iterations with a relative error of 0.1802 for 20% of Gaussian noise and for the same scheme the existing CGLS method has a 0.4480 relative error at the 77 iterations. Further, the FP-CGLS along with the DBIM method produces a reconstructed image with the accuracy of 0.8760 in four DBIM iterations.

Index Terms **–** CGLS, ill-posedness, Krylov subspace method, microwave tomography, regularization.

I. INTRODUCTION

Microwave Tomography Imaging System (MwTIS) is a promising diagnostic tool in breast cancer detection [1] and monitoring [2, 3] its progress towards widespread clinical application. It inspires several benefits such as usage of nonionizing low power electromagnetic signals, cost-effective antenna-array, low health risk, and portability. MwTIS aims at estimating the dielectric values of internal tissues from processing measured electromagnetic field data is stated to solve the electromagnetic inverse scattering problem [4]. Various inverse scattering problem resolving algorithms such as the Born iterative method (BIM), Distorted Born iterative method (DBIM), and Gauss Newton (GN) can employ to compute images by a set of underdetermined linear equations. Every iteration of the DBIM algorithm, the linear system of equations is solved by using regularization methods and has found optimal solutions by the inversion process. Thresholding [5, 6], Compressive sensing with Sparsity [7], and Krylov subspace-based methods [8] are explored towards the quality of the resultant image.

Refinement of image resolution and reduction of computation time is currently needed in medical diagnosis applications for microwave imaging. While incorporating prior information [9], reducing the size of resolution grid elements [10], contrast enhancement [11], and high frequency microwaves [12] certainly increased the quality of microwave tomography images. High frequencies in MwTIS have inherently obtained fine internal details of the tissues in a high resolution grid than low frequency. Although high frequency microwave has increased the spatial resolution that may be acquired in high resolution images, unstable convergence is a significant limiting factor in the inversion process. The multifrequency [6, 13] approach has stabilized the inversion process by reducing the imbalance ratio between the number of measurements and the number of pixels in high resolution grid. Hence, this paper has conducted a detailed study and proposed a method to improve significant resolution enhancement with multifrequency in breast imaging systems. Excellent imaging results have been obtained using frequency hopping techniques which is an initial guess pursued by inverting single-frequency data then followed by processing of multifrequency data. This can be extremely time-consuming due to non-linearity raised by the frequency diversity problem (switching from low frequency to high frequency) and ill-posedness in the linear system of equations. A credible work in the literature, DBIM with Thresholding method [6] and wavelet basis with CGLS method [14] resolved the above problem by hybrid frequency hopping technique. It is performed well

Submitted On: April 14, 2022
Accepted On: June 27, 2022

https://doi.org/10.13052/2022.ACES.J.370602

in the resolution of 1 mm to 4 mm but they lacked to perform below 1 mm resolution breast images. Because, each frequency range has its unique characteristics like convergence time, stability in solution estimation, and also put in high measurement noise in the received scattered fields. Further, it meets more computational burdens like a greater number of iterations to construct sufficiently high-resolution images. Therefore, this paper gives special attention to the multifrequency techniques and regularization method to handle nonlinearity and ill-posedness problems in the reconstruction algorithm.

This paper proposed two schemes to resolve the above-mentioned problems in DBIM with a multifrequency microwave tomography breast imaging system. The first is reducing the nonlinearity by selecting the optimal step frequency in frequency hopping techniques. The value called degree of ill-posedness helps to select the suitable step frequency which makes the minimum effects of ill-posedness in the linear system of equations. The second scheme is proposing a Preconditioner incorporating the Krylov subspace regularization method to achieve optimal imaging accuracy and reconstruction stability by solving the ill-posedness problem. Conjugate Gradient Least Square (CGLS) is one of the credible Krylov subspace regularization methods that worked well with the DBIM reconstruction algorithm for tumor detection [15] and density estimation [16] in breast imaging applications. This paper proposed a modified version of the CGLS method called the Flexible Preconditioner CGLS (FP-CGLS) method for inverting underdetermined multifrequency linear equations with high measurement error. In this proposed scheme, the Flexible Preconditioner is being updated in every iteration helps to stable and quicken the convergence time in an unstable high-frequency imaging system. In addition, the non-negativity constraint in the estimation of the appropriate dielectric values of unknown breast tissues is increases the truthfulness of the solution. These proposed schemes take less iteration for the DBIM algorithm to find the high accuracy resultant images.

The paper is organized into the following sections. Section 2 explains the measurement matrix formation process. A detailed description of the proposed method is stated in section 3. Section 4 explained the properties of breast phantom, implementation specifications, and the results achieved from the study. The conclusion is explained in section 5.

II. MEASUREMENT MATRIX FORMULATION

This section explains the formation of a measurement matrix based on the design characteristics of the MwTIS. The circular measurement domain (S) with the transmitter (N_t) and receiver (N_r) antennas and the object are present in the D domain. The object is illuminated by the N_t and the scattered fields are received by the N_r simultaneously. The integral equation of imaging domain (D) linearized by the first-order Born approximation which governs the entire DBIM algorithm expressed in eqn (1),

$$E_{scat}(r) = k_b^2 \int_d \mathrm{G}(\mathrm{r},\mathrm{r}^{'}).X_{object}(r^{'})E_{inc}(r^{'})dr^{'}. \quad (1)$$

$\mathrm{G}(\mathrm{r},\mathrm{r}^{'})$ is the Green's function with the wavenumber of the background medium (k_b). $X_{object}(r^{'})$ is relative permittivity $(\frac{\varepsilon_r-\varepsilon_b}{\varepsilon_b})$ of an object to be imaged. E_{inci} is the plane wave incident fields. $\mathrm{r}^{'},\mathrm{r}$ are the spatial positions in S and D domains. To format the measurement matrix of the proposed work, integral (1) of the imaging domain is discretized using Fredholm of the first kind and pixel-based smooth basis function [17]. It leads to an increase the imaging accuracy as well as resolution. Now, the integral equation (1) is converted into a linear system of equations as,

$$A_{MxN}.X_{Nx1} = b_{Mx1}. \quad (2)$$

Here $\boldsymbol{A}_{(M\ X\ N)}$ is the measurement matrix which is the outcomes of the interaction between the incident field and background medium. $\boldsymbol{b}_{MX1}$ is the received scattered field. Here M is the number of measurement antenna pairs and N is the row vector representation of the number of pixels in the image grid. In the multifrequency forward process, the size becomes $(M\ X\ F)\ X\ N)$. Here F is the number of frequencies in the multifrequency range.

III. PROPOSED ENHANCEMENT SCHEME FOR MICROWAVE BREAST IMAGING

A. Proposed optimized step frequency to resolve frequency diversity problem

This section has detailed the behavior of condition number in the system measurement matrix (**A**) due to variation in the operating frequency value and selection of optimum multifrequency range with minimum condition number. The performance of the reconstruction algorithms is based on the condition number of the system coefficient matrix (**A**). Small changes in the condition number of **A** will affect more in the solution more. It takes more iteration to converge the solution and struggle to produce the appropriate solution. This is called an ill-posed condition problem. In this paper, a study has been conducted to analyse the impact of the frequency diversity problem in the existing studies [6, 14]. It depicts, that the condition value increases in the multifrequency range due to the high frequency hopping step from 1 GHz to 3 GHz To meet the high spatial resolution requirement of MwTIS, the paper needs to find the optimum multifrequency scenario with a high frequency range. So, the measurement matrix (A) of the proposed multifrequency needs to estimate the effect of ill-posedness on the frequency diversity problem. The factor called degree of

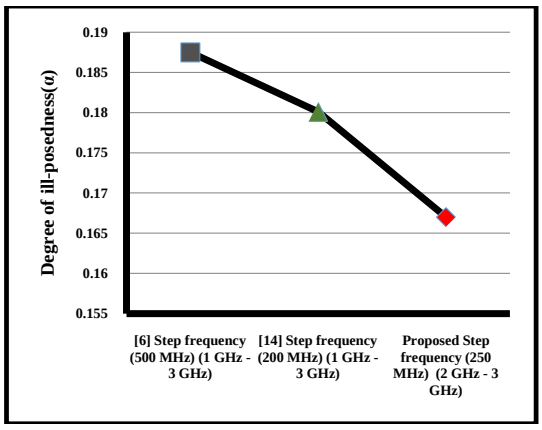

Fig. 1. Analysis of α value for the proposed multifrequency scenario in high frequency range.

ill-posedness (α) value [18] was used to find the proposed multifrequency scenario. It is calculated using,

$$\mathrm{K(A)} = \exp(-\alpha.\mathrm{i})\,. \tag{3}$$

Here, K(A) is the condition number of A and i is the number of the singular value spectrum. α is the positive integer value. The α is calculated for two different step frequencies such as 500 MHz [6] and 200 MHz [14] in the 1 GHz to 3 GHz frequency range. As well, α is calculated for the 250 MHz jumping frequency for the proposed multifrequency range from 2 GHz to 3 GHz These values are plotted in Fig. 1. It has shown that the proposed frequency has a minimum α value than the existing scenario. Based on the above analysis the suitable frequency range for the desired application can be fixed. Further, this analytical proof has depicted the proposed multifrequency scenario will produce a good quality image in the regularization process. However, the measurement matrix (A) in eqn (2) is under-determined and needs to solve by the normal equation in the least square method such as the CGLS method. A detailed explanation of the solving procedure of A is stated in the next section.

B. Proposed flexible preconditioned CGLS (FP-CGLS) regularization method

This section has explained the steps and advantages of the proposed Flexible Preconditioned CGLS (FP-CGLS) Krylov subspace regularization method. Especially in medical imaging, Born (BIM, DBIM) type reconstruction algorithms give under-determined $((M\ X\ F) << N)$ set of linear equations which means the imbalance between $(M\ X\ F)$ and (N). The cost function is represented as,

$$\min \phi(x) = A^T Ax = A^T b. \tag{4}$$

The results from the analytical study in section 3.1 depict the A having α as 0.169 and it conveys the A is stuck with the ill-posedness problem. Due to the large condition number of A, the right-hand side b is contaminated by noise (b+ $\dot{\eta}$) in real-time. Eqn (4) solved using CGLS may compute the useless solution and often converge very slowly and cannot stable in the number of iterations in frequency diversity problem in the multifrequency scenario. To resolve the above problem, one needs additional computational matrix called preconditioner (P) is added to eqn (4). The linear equations become,

$$\min \phi(x) = P^{-H} A^T A P^{-1} x - P^{-H} A^T b. \tag{5}$$

Here, P $\in$ $\mathrm{R^{N\ x\ N}}$. In this paper, the Krylov subspace method called Flexible Preconditioner CGLS method is taken to solve eqn (5). It is an enhanced version of the PCGLS [19] method. It is used to estimate dielectric values of x by fast convergence in ill-condition A and appropriate x in noise is corrupted in the received scattered field. It increases the accuracy and reduces the number of iterations compared to the standard solvers. To compute the meaning solution one additional constraint called non-negativity is added in this method. The appropriate solution $x_{\boldsymbol{m}}$ in standard CGLS is determined as follows,

$$x_m = x_{m-1} + \alpha_{m-1}.d_m. \tag{6}$$

In FP-CGLS the parameters such as scalar step length (α_{m}) and the direction vector ($\mathrm{d_m}$) enforce non-negativity in every iteration

$$\alpha_{m-1} = \frac{(res_{m-1}, w_{m-1})}{(w_{m-1}, w_{m-1})}. \tag{7}$$

Here m is the iteration index. $\alpha_{\mathrm{m-1}}$ selected by satisfying the bounded step length $\overline{\alpha_{\mathrm{m-1}}}$ condition $\overline{\alpha_{\mathrm{m-1}}}$>0. The bounded step length is computed as follows,

$$\overline{\alpha_{m-1}} = \min(\alpha_{m-1}, \min(\frac{-x_{m-1}(d_{m-1} < 0)}{d_{m-1}(d_{m-1} < 0)})). \tag{8}$$

The scalar $\overline{\alpha_{\mathrm{m-1}}}$ is satisfies the condition of orthogonality which project the $\mathrm{A^T b}$ in the nonnegative orthant, due to $\mathrm{x_{\boldsymbol{m}}}$= 0 until the $\overline{\alpha_{\mathrm{m-1}}}$>0. It gives added truthfulness to the solution in which the imaged object does not contain negative dielectric properties. The iteration depends on the residual norm vector $res = \left(b + \dot{\eta}\right) - \mathrm{A.x_{\boldsymbol{m}}}$ and $\mathrm{d_m}$. To improve the speed of convergence the left preconditioner $(\mathrm{P_m})$ is multiplied to $\mathrm{res_m}$. It is computed as follows,

$$P_m = P_m A^T res_m. \tag{9}$$

The standard PCGLS method calculated the L as a $(N\ X\ N)$ sparse matrix but in the proposed FP-CGLS the $\mathrm{P^{(m)}}$= diag($\mathrm{x_m}$) and it is updated in every iteration. Every iteration step ensures the nonnegativity constraints and proceeds right direction towards the appropriate subspace. So that it is called as Flexible Preconditioner CGLS method. This is the reason the solution x does not distort by the measurement noise ($\dot{\eta}$). The cost of

computing vector and matrix multiplication with a preconditioner is minimum compared to other Krylov methods like CGLS. The residual norm is set as the stopping criteria. The discrepancy principal inequality condition helps to stop the iteration at right time. The FP-CGLS does not require an explicit regularization parameter instead of that the step length (α) and tuning parameter (β) do the same. In this manner, the proposed FP-CGLS method controls the measurement error and unstable convergence due to the frequency diversity problem by resolving the ill-condition problem with less number of iterations. It improves the quality of high-resolution MWTIS for the breast category.

IV. RESULTS AND DISCUSSION

This section has explained the numerical setting of the simulation study and evaluated the results achieved by the proposed FP-CGLS method for desired multifrequency scenario using scattered breast phantoms. The main purposes of the study have mentioned below,

- Analysed the reconstruction performance of the proposed multifrequency range 2 GHz to 3 GHz with 250 MHz step frequency using the proposed FP-CGLS. The relative error and optimal iteration count are used to evaluate the performance.
- The convergence behavior of the proposed FP-CGLS is examined by adding different measurement error levels ($\dot{\eta}$) in the scattered field (b) that are $\dot{\eta} = 10\%,\ 20\%$, and 30%. The relative residual norm and iteration count are the parameters used for the convergence analysis.
- The efficiency of the FP-CGLS in the DBIM reconstruction algorithm is analyzed by the Mean Square Error (MSE) and DBIM iteration count.

The simulation study has also been conducted by the standard CGLS method for comparative analysis.

A. Simulation specification and dataset

The circular imaging system (domain S) is set with a diameter of 30 cm The $N_t = 15$ and $N_r = 16$ are placed around the boundary of the S domain. In the real-time scenario, the breast was immersed in a lossless coupling medium, for that the background medium is assigned to $\varepsilon_b = 2.6$ in the proposed method. The $M = 240$ samples of scattered fields are collected by consecutive incidence and reception of these N_t and N_r. The five equally spaced ($F = 5$) multifrequency scenarios are in the range of 2 GHz to 3 GHz (proposed in section 3.1). The numerical process and evaluation were done in MATLAB-R2021. The Scattered (ID=070604PA1) breast phantom has been taken from the numerical repository of the Cross-Disciplinary Electromagnetics Laboratory [20] (University of Wisconsin CEM Laboratory) for the proposed work. The 2D slice No 135 of the phantom is extracted from the 3D breast model.

The breast phantom is shown in Fig. 2. The pixel size is equal to 0.5 mm and other prerequisite data are initialized as mentioned in the instruction manual [20] of the same. The dielectric values of the breast tissues [21] in the phantoms are listed in Table 1. The numerical process and evaluation were done in MATLAB-R2021.

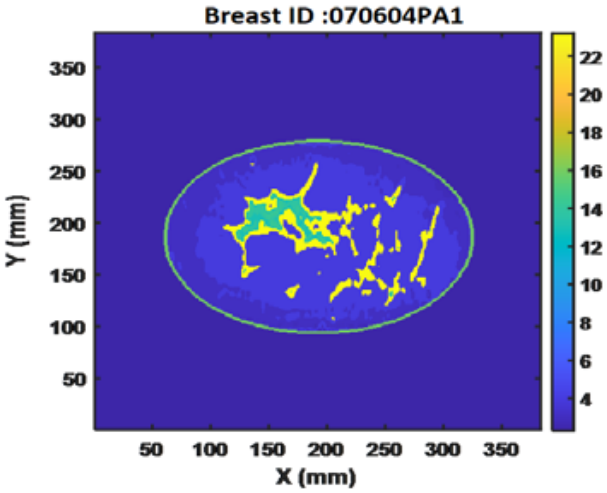

Fig. 2. Reference scattered breast phantom.

Table 1: Debye parameters of the breast tissues: [21]

Material	ε_∞	$\triangle\varepsilon$	σ_s
Adipose	3.987	3.545	0.080
Fibrogland	13.91	40.49	0.824
Background medium	2.6	0.092	0.005
Skin	15.93	23.83	0.831

B. Assessment of proposed FP-CGLS in desired multifrequency range

This section has explained the performance of the proposed multifrequency range using the FP-CGLS method in the reconstructed breast phantoms. The below-mentioned results are taken at A matrix of size (1280×146689). The reconstruction quality of the proposed FP-CGLS method and the parameters like Relative Error and total iteration ($Iter$), the count is compared with CGLS. In this study, the maximum iteration count is set as 150 and $\dot{\eta}$=0 to compare the performance of these two methods. The calculation of Relative Error (RE) as follows,

$$RE = \frac{||X(r') - x_m||_2}{||X(r')||_2}. \tag{10}$$

Table 2: Comparison of relative error and their optimal stopping iterations for proposed FP-CGLS

Breast phantom	Methods	*Iter*	*RE*
Scattered Breast ID:070604PA1	FP-CGLS	18	0.1770
	CGLS	77	0.4480

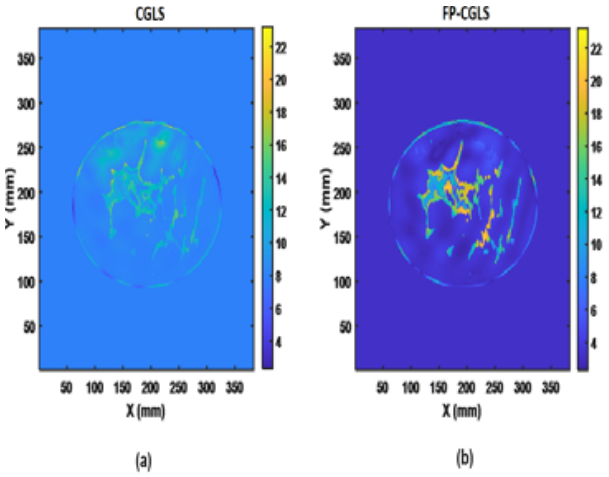

Fig. 3. Reconstructed images of CGLS and proposed FP-CGLS method using multifrequency range 2 GHz to 3 GHz.

The best iteration count is selected by the discrepancy principle and listed in Table 2. This result has been achieved in the single DBIM iteration. The results in Table 2 clearly explained the benefits of the preconditioner (P_m) in the FP-CGLS methods.

The FP-CGLS method has achieved a minimum relative error of 0.1773 within 18 iterations. Further CGLS method has required 77 iterations to reach the minimum relative error value of 0.4480. The reason behind this is the FP-CGLS regularization method effectively quickens the slow convergence of the gradient in the CGLS method. Note that, the proposed FP-CGLS produces a better result with the minimum number of iterations for the proposed high frequency multifrequency range microwave tomography imaging system. The reconstructed image of the final DBIM iterations is shown in Fig. 3. Assessment of Proposed FP-CGLS Convergence on Gaussian Noise This section has explained the convergence behavior of the proposed FP-CGLS regularization method by varying the different Gaussian noise levels.

Computing the differences in Relative Residual Norm (***RR_Norm***) for newly estimated x in successive iterations is called convergence analysis. It shows how the algorithms are moved closer to the desired solution. In this study, the Gaussian noise model is used to simulate the error vector of three distinct noise levels that are $\dot{\eta} = 10, 20,\ 30\%$.

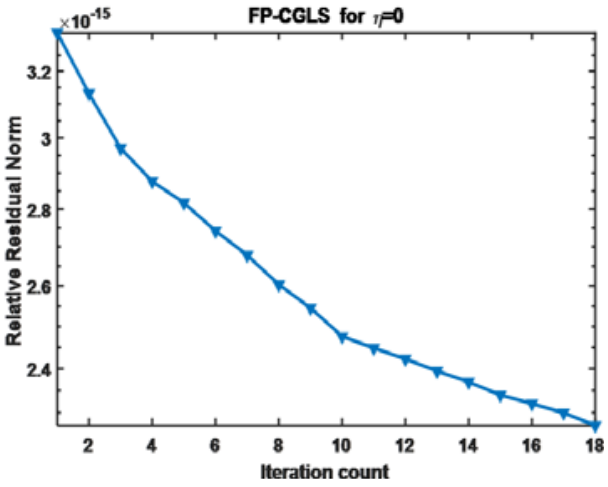

Fig. 4. Convergence plot for the reconstructions of the scattered breast using proposed FP-CGLS method.

It is added to b in eqn (2). This approach is used to test the stability and robustness of the regularization method against uncertainties like noise and other artifacts in the measurement system. The calculation of relative residual norm is calculated as,

$$RR\_Norm = \frac{||A^T d_m - x_m||}{||A^T b||_2}. \tag{11}$$

The semi-log plot of Relative Residual Norm (***RR_Norm***) and iteration count helps to numerically analyze the convergence behavior of the proposed solution based Preconditioner ($\mathbf{P_m}$). Figures 4 and 5 show the semilog plot for the CGLS method and proposed FP-CGLS method. These figures are show the convergence of these two regularization methods without noise distortion. The noticeable value in this plot is the magnitude of *RR_Norm*.

The FP-CGLS method reaches the minimum value ($\mathbf{10^{-15}}$) at the beginning of the iteration, But CGLS method reached $\mathbf{10^{-4}}$ only at the end of the iteration.

The product of $\mathbf{P_m}$ with $\mathbf{res_m}$ quickly move to the negative descent direction. Figure 6 shows the comparison plot between FP-CGLS and CGLS regularization methods for the different noise levels. The increments in noise level reduce the iteration count in both FP-CGLS and CGLS methods, but the FP-CGLS method is stable in convergence (12 iterations) up to 20% of noise distortion. The CGLS has sudden fall from 77 iterations to 17 iterations in 20% of noise distortion.

The relative error value and the number of iterations are recorded for the FP-CGLS and CGLS methods for the three noise levels are listed in Table 3. It shows that FP-CGLS has a substantially higher measurement

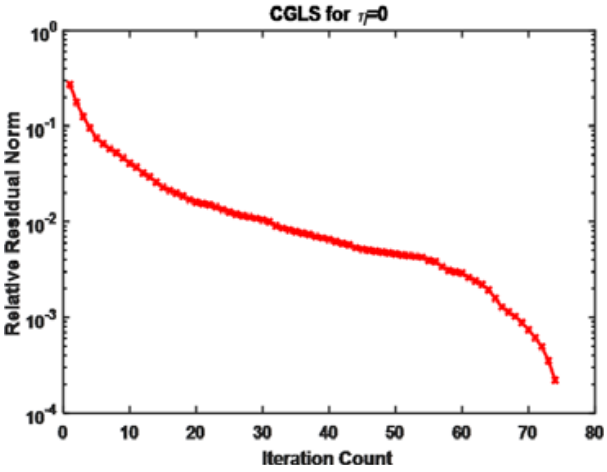

Fig. 5. Convergence plot for the reconstructions of the scattered breast using CGLS method.

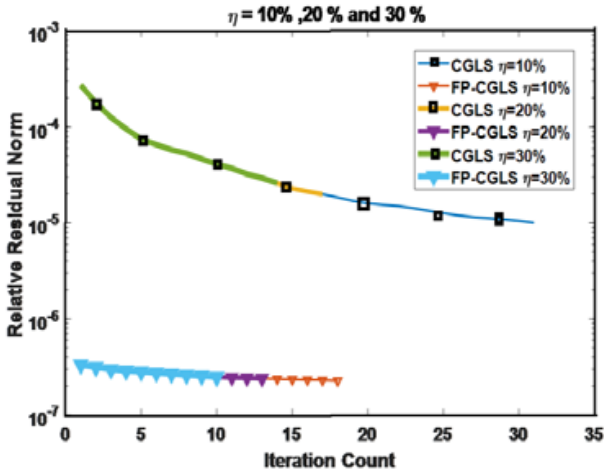

Fig. 6. Comparison of relative residual norm versus iteration count for the $\dot{\eta}$ = 10%, 20%, and 30% for FPCGLS and CGLS methods.

error handling ability than the CGLS method in $\dot{\eta}$ up to 20% except for the error level $\dot{\eta}$=**30**%. There is a minor increment in the relative error value. Another observation is, that the CGLS method stuck into stagnation problem even though in $\dot{\eta}$= **20**%. Based on the results, FP-CGLS has stable convergence behavior in higher measurement error.

C. Assessment of proposed FP-CGLS on DBIM

This section has explained the overall reconstruction performance of the DBIM algorithm combined with the proposed FP-CGLS method for the desired multifrequency range in a scattered breast phantom. The results are taken at A matrix of size (1280 × 146689). The $\dot{\eta}$ is set as 0. The pixel size is assigned as 0.5 mm for high resolution reconstructed image. A cross-section plot (Fig. 7) of the reconstructed image illustrates the goodness of the proposed FP-CGLS method. It is plotted between the spatial position on X-axis and its corresponding static relative permittivity values on Y-axis. These types of visualization help to identify the estimated dielectric values of the reconstructed image have met the actual values in the reference breast phantom. Figure 7 shows the reconstructed image in the second and fourth iteration of the iteration of the DBIM algorithm along with the reference profile. It showed the proposed FP-CGLS produces an appropriate result in 4 DBIM iterations. It has achieved accuracy values 0.6030, 0.6936, 0.7665, 0.8760 in DBIM iteration 1, 2, 3 and 4 respectively. According to this analysis, the proposed FP-CGLS method is performed well in the high frequencies in multifrequency microwave tomography breast imaging even though in higher noise levels.

Table 3: Comparison of relative error and their optimal stopping iterations for different Gaussian noise

Methods	$\dot{\eta}$=**10**%		$\dot{\eta}$=**20**%		$\dot{\eta}$=**30**%	
	Iter	*RE*	*Iter*	*RE*	*Iter*	*RE*
FP-CGLS	17	0.1773	12	0.1802	10	0.2215
CGLS	31	0.4755	17	0.4992	13	0.51865

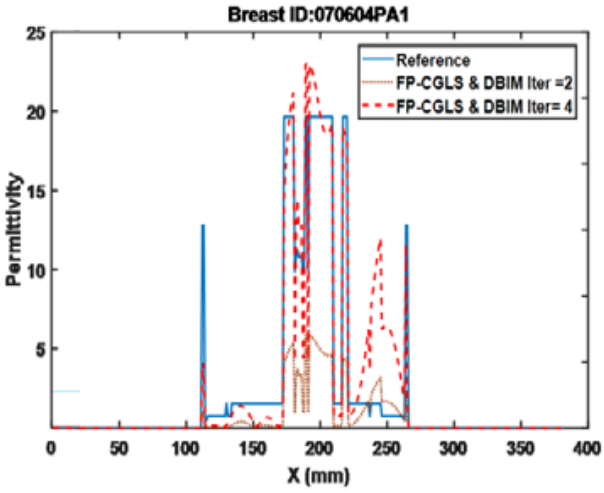

Fig. 7. Cross-sectional view of reconstructed permittivity of scattered breast using proposed FP-CGLS with iteration of DBIM algorithm.

V. CONCLUSION

This paper presents the high frequencies in multifrequency DBIM with a proposed Krylov subspace based regularization method called FP-CGLS for high-

resolution MWTIS breast imaging. The frequency diversity problem is a major issue in multifrequency microwave tomography imaging. It leads to received scattered fields corrupted by Gaussian noise and unstable convergence in the reconstruction process. This paper addresses these issues modelled as the ill-condition problem. It was resolved by the proposed optimal step frequency (250 MHz) for the high frequency range (2 GHz to 3 GHz) selected based on the degree of ill-posedness value. The unstable convergence and accuracy of the solution are resolved by the iteratively updated preconditioner based FP-CGLS method. A scattered breast phantom has been taken for this study. Stand CGLS method is used to compare the performance of the proposed multifrequency and FP-CGLS method. The iteratively updated preconditioner P_m in the proposed FP-CGLS method supports reaching the appropriate x_m at 12 iterations with a relative error of 0.1802 even though in 20% of Gaussian noise. Compare the results with the Standard CGLS method; it achieved a 0.4480 relative error value at the 77 iterations. The FP-CGLS along with the DBIM method produces a reconstructed image with the accuracy of 0.8760 in 4 DBIM iterations.

ACKNOWLEDGMENT

This work was supported by the Thiagarajar Research Fellowship (TRF) scheme in Thiagarajar College of Engineering, Madurai.

REFERENCES

[1] N. Abdollahi, I. Jeffrey, and J. LoVetri, "Improved tumor detection via quantitative microwave breast imaging using eigenfunction-based prior," *IEEE Trans. Comput. Imaging*, vol. 6, pp. 1194-1202, 2020.

[2] B. Oliveira, D. Godinho, M. O'Halloran, M. Glavin, E. Jones, and R. Conceição, "Diagnosing breast cancer with microwave technology: Remaining challenges and potential solutions with machine learning," *Diagnostics*, vol. 8, no. 2, pp. 1-22, 2018.

[3] G. Boverman, C. E. L. Davis, S. D. Geimer, and P. M. Meaney, "Image registration for microwave tomography of the breast using priors from nonsimultaneous previous magnetic resonance images," *IEEE J. Electromagn. RF Microwaves Med. Biol.*, vol. 2, no. 1, pp. 2-9, Mar. 2018.

[4] Semenov, "Microwave tomography: Review of the progress towards clinical application," *Philos. Trans. A. Math Phys. Eng. Sci.*, vol. 367, pp. 3021-3042, 2009.

[5] M. Ambrosanio, P. Kosmas, and V. Pascazio, "A multithreshold iterative DBIM-based algorithm for the imaging of heterogeneous breast tissues," *IEEE Trans. Biomed. Eng.*, vol. 66, no. 2, pp. 509-520, 2019.

[6] Z. Miao and P. Kosmas, "Multiple-frequency DBIM-TwIST algorithm for microwave breast imaging," *IEEE Trans. Antennas Propag.*, vol. 65, no. 5, pp. 2507-2516, 2017.

[7] M. Azghani, P. Kosmas, and F. Marvasti, "Fast microwave medical imaging based on iterative smoothed adaptive thresholding," *IEEE Antennas Wirel. Propag. Lett.*, vol. 14, pp. 438-441, 2015.

[8] H. Harada, D. J. N. Wall, T. Takenaka, and M. Tanaka, "Conjugate gradient method applied to inverse scattering problem," *IEEE Trans. Antennas Propag*., vol. 43, no. 8, pp. 784-792, 1995.

[9] L. M. Neira, B. D. Van Veen, and S. C. Hagness, "High-resolution microwave breast imaging using a 3-d inverse scattering algorithm with a variable-strength spatial prior constraint," *IEEE Trans. Antennas Propag.*, vol. 65, no. 11, pp. 6002-6014, Nov. 2017.

[10] Y. Suzuki and S. Kidera, "Resolution enhanced distorted born iterative method using ROI limiting scheme for microwave breast imaging," *IEEE J. Electromagn. RF Microwaves Med. Biol.*, vol. 5, no. 4, pp. 379-385, 2021.

[11] M. T. Bevacqua and R. Scapaticci, "A compressive sensing approach for 3D breast cancer microwave imaging with magnetic nanoparticles as contrast agent," *IEEE Trans. Med. Imag*, vol. 35, no. 2, pp. 665-673, Feb. 2016.

[12] M. A. Aldhaeebi, K. Alzoubi, T. S. Almoneef, S. M. Bamatraf, H. Attia, and O. M. Ramahi, "Review of microwaves techniques for breast cancer detection," *Sensors*, vol. 20, no. 390, pp. 1-38, 2020.

[13] C. Kaye, I. Jeffrey, and J. LoVetri, "Improvement of multi-frequency microwave breast imaging through frequency cycling and tissue-dependent mapping," *IEEE Trans. Antennas Propag.*, vol. 67, no. 11, pp. 7087-7096, Nov. 2019.

[14] R. Scapaticci, P. Kosmas, and L. Crocco, "Wavelet-based regularization for robust microwave imaging in medical applications," *IEEE Trans. Biomed. Eng.*, vol. 62, no. 4, pp. 1195-1202, 2015.

[15] T. Rubaek, P. M. Meaney, P. Meincke, and K. D. Paulsen, "Nonlinear microwave imaging for breast-cancer screening using Gauss-Newton's method and the CGLS inversion algorithm," *IEEE Trans. Antennas Propag.,* vol. 55, no. 8, pp. 2320-2331, 2007.

[16] J. D. Shea, P. Kosmas, S. C. Hagness, and B. D. Van Veen. "Three-dimensional microwave imaging of realistic numerical breast phantoms via a multiple-frequency inverse scattering technique," *Medical Phys*., vol. 37, no. 8, pp. 4210-4226, 2010.

[17] D. W. Winters, J. D. Shea, P. Kosmas, B. D. Van Veen, and S. C. Hagness, "Three-dimensional

microwave breast imaging: Dispersive dielectric properties estimation using patient-specific basis functions," *IEEE Trans. Med. Imaging*, vol. 28, no. 7, pp. 969-981, 2009.

[18] Q. Fang, P. M. Meaney, and K. D. Paulsen, "Singular value analysis of the Jacobian matrix in microwave image reconstruction," *IEEE Trans. Antennas Propag.*, vol. 54, no. 8, pp. 2371-2380, Aug. 2006.

[19] S. Gazzola, "Fast nonnegative least squares through flexible Krylov subspaces," *SIAM J. Sci. Comput.*, vol. 39, pp. A655-A679, 2017.

[20] Available from https://uwcem.ece.wisc.edu/phantomRepository.html

[21] P. T. Nguyen, A. Abbosh, and S. Crozier, "Microwave hyperthermia for breast cancer treatment using electromagnetic and thermal focusing tested on realistic breast models and antenna arrays," *IEEE Trans. Antennas Propag.*, vol. 63, no. 10, pp. 4426-4434, Oct. 2015.

N. Nithya received the B.E. degree in computer science and engineering from Anna University, Tamilnadu, India, in 2009 and the M.E. degree in computer science and engineering from Anna University, Tamilnadu, India, in 2014. She is currently pursuing the Ph.D. degree in Information and Communication at Anna University, Tamilnadu, India from 2017 to 2020. From 2015 to 2018, she was a Assistant Professor in the Department of computer science and engineering. Her current research interests include microwave tomography imaging, inverse problems techniques, regularization method for the breast cancer detection and brain stroke microwave imaging, ill-posed and ill-condition problems in linear equation.

M. S. K. Manikandan received the BE degree in Electronics and communication engineering from NIT-Trichy, Tamilnadu, India,in 1998 and the ME degree in communication systems from Thiagarajar College of Engineering, Tamilnadu, India in 2000. He completed Ph.D in Information and communication at Anna University, Tamilnadu, India in 2010. Since 2001 he has been an faculty with Electronics and communication engineering department, Thiagarajar College of Engineering. He is the author of more the 25 articles in reputed journals and conference. His research interests include wireless communication and medical image analysis.